www.gondwanags.org.in

Original Article

ISSN : 2455-1953

JGSR
Journal of Geosciences Research
Vol. 7, No.2, July, 2022, pp. 193-201

Genesis of Cobalt Mineralisation Associated With Kalyadi Schist Belt, Dharwar Craton, South India: A Petrological and Fluid Inclusion Study

Mahantesha P.[1]*, K.N. Prakash Narasimha[2], M. Shareef [3], G. Gopalakrishna[4], Girish Kumar Mayachar[4], S.S.A. Rasool[4], Aneesh S.S.[4] and T.K.A. Rahim[5]

[1]*Geological Survey of India, SU:K and G, Bengaluru, Karnataka- 560111(KN), India*
[2]*Department of Studies in Earth Science, University of Mysore, Manasagangotri, Mysore- 570006 (KN), India*
[3]*Geological Survey of India, FTC, Chitradurga -577502 (KN), India*
[4]*Geological Survey of India, NCEGR, Bengaluru -560111 (KN), India*
[5]*Hatti Goldmines Ltd., Raichur -584115 (KN), India*
*(*Corresponding author, E-mail: mantugeo11@gmail.com)*

Abstract

The Sargur Group of rocks belonging to the Kalyadi Schist Belt (KSB) in the Western Dharwar Craton (WDC) occur as large linear enclaves within younger peninsular gneisses. This belt is known for copper mineralization and exploited good amount of copper for many years. Recent studies have shown significant concentration of cobalt up to 2000 ppm associated with copper in this belt. Earlier studies have indicated pyrite containing cobalt in its crystal lattice. In the present study an attempt has been made to understand the genesis of cobalt mineralization in this belt through detailed petrography, fluid inclusion studies along with chlorite chemistry. Two distinct ore mineral assemblages and fluid sources are proposed based on ore petrography, mineral chemistry and fluid inclusion studies. In the initial stage chalcopyrite1 is associated with cobalt bearing pyrite and magnetite and in the later stage chalcopyrite2 is associated with arsenopyrite, pyrrhotite and safflorite [(Co, As) As_2]. The initial stage fluids are characterized by low saline (~ 5 wt % NaCl equivalent) and slightly higher temperature (268° to 300° C with pressure ranging from 1.9 to 2.3 Kb), which are almost similar to temperatures obtained from the chlorite *i.e.* 202.8° to 322.43° C, this indicates that the fluids are related to regional low grade greenschist facies metamorphism. On the contrary, the late stage fluids are characterized by high density and high saline nature and show temperature range varying from162° to 224° C with pressure values ranging from 1.4 to 1.9 Kb and in addition native Bi association suggest their derivation from the granitic or felsic magmatic source associated with emplacement of the Desani Granite in the study area. Presence of safflorite mineral associated with the second stage fluids and mineral assemblage suggest that the remobilization Co from the crystal lattice of pyrite and chalcopyrite has occurred.

Keywords: Cobalt mineralisation, Sargur Group of Rocks, Kalyadi Schist Belt (KSB), Western Dharwar Craton

Introduction

Cobalt occurrences in India are very limited and it has received less attention. No individual deposit has been reported till date and even if concentrations are high, never assumed importance. Due to its strategic importance and occurrence of no major deposits, large input of Co to our country is due to the import from Africa, Australia and China. In the present context, it is always seen as a by-product of the polymetallic deposits of different Cratonic parts *viz.*, Dharwar, Aravalli, Bastar and Singhbum. Genetically Co is associated with Cu, Ni, other base metal and gold in Volcanogenic massive sulphides (VMS)-Ingaldhal and Kalyadi in Karnataka (Mookherjee and Philip, 1979), Iron Oxide – Copper – Gold type (IOCG)–Khetri in Rajasthan and Thanewasna Copper Deposit from the Western Baster Craton (Dora *et al.*, 2017), Magmatic Ni-Co-PGE association and laterites of mafic ultramafic series , Banasandra in Karnataka (unpublished report of GSI from FSP: 2019-21), Cobalt-Bearing Grunerite in the Metamorphosed Banded Iron Formation in Gorumahisani-Sulaipat-Badampahar Belt in the east of North Orissa Craton (Nayak, 2011) and Volcanogenic exhalative (Ni-Co-As-S Singhbhum Copper Belt) are some of the geological occurrences of the Cobalt mineralization in India.

Among the earliest known occurrence, Kalyadi Cu-Co deposit is prominent, being mined only for Cu having concentration up to 1 %. Even though Co reserves of 5.8 Mt with 650ppm cut of grade has been reported from this deposit (Paremeswaraiah, 1996; Krishna Rao, 1998), but no further work assumed significance. Earlier workers have highlighted Cu mineralization and its genesis (Ravindra *et al.*, 1990; SubbaRao and Naqvi, 1997; Abdul Rahim and Nijagunappa, 2001). Studies have shown Co concentration up to 3297 ppm associated with mainly pyrite, whereas main Cu ore *i.e.* chalcopyrite contains Co up to 93 ppm (Subba Rao and Naqvi, 1997; Krishna Rao, 1998; Thomas, 2006). Co is present in the crystal lattice of pyrite without any specific Co mineral phases in general (Krishna Rao, 1998; Thomas, 2006). No significant work

(Received : 11 October 2021 ; Revised Form Accepted : 25 March 2022)
https://doi.org/10.56153/g19088-021-0064-6

has been carried out to understand the genesis aspect of Co in particular. Recent studies by Mahantesha *et al.* (2021) have reported Co values up to 2000 ppm from the pyrite-chalcopyrite zones in quartzite and metavolcanic rocks. Considering the concentration of Co in association with the Cu ore, in the present study various tools such as petrography, XRD, SEM, EPMA and micro-thermometrystudies were utilized to emphasise the genesis of Co mineralization associated with the Kalyadi Copper Deposit. The present study focuses on the role of fluids, P-T condition of Co mineralization in Kalyadi with a scope for further exploration activities in the Dharwar Craton.

Geological Settings and Mineralisation

The Kalyadi Copper-Cobalt Deposit is located in the Western Dharwar Craton (WDC) associated with NNW-SSE trending the Kalyadi Schist Belt (KSB) consists of Sargur Group of rocks. This older volcano-sedimentary sequence is present within the intrusive peninsular gneisses (Fig.1a-b). Many workers consider this belt as part of Nuggihalli and Holenarsipur schist belts (Bhaskar Rao, and Venkataraman, 1982; Ravindra *et al.*, 1990). The common rock types in the Kalyadi Schist Belt (KSB) are quartzite, meta-ultramafite and amphibolite formed under upper greenschists to middle amphibolite facies metamorphism (Fig.2). The study area has undergone three distinct phases of deformation. Well-developed schistosity is defined by strong mineral alignment, tight isoclinal folds (F1) at places rootless in nature defines D1 deformation. D2 structures are dominant with open fold geometry with spaced and crenulation cleavage with trends in NNW-SSE direction and sub vertical easterly dips, whereas D_3 deformation is represented by broad warps.

Cu-Co mineralization in the KSB is hosted by quartzite and metavolcanic rocks. The Cu mineralization is considered by earlier workers as syngenetic stratiform and sedimentary exhalative origin (Ravindra *et al.*, 1990; Subba Rao and Naqvi, 1997). The chalcopyrite is the main ore mineral of copper, whilst Co concentration is associated with the early pyrite crystals (Krishna Rao, 1998; Thomas, 2006) in the KSB. Mineralized zone is about 600m and trends in N15 to 40° W strike direction with an average width of 30m.

Encrustation of Malachite and Azurite on surface as well as occurrence of visible sulphides in the form of stringers of chalcopyrite, pyrrhotite and pyrite are observed (Fig. 3b). Mineralized zones show intense wall rock alteration and quartz-carbonate vein activity parallel to strike of the host rocks. Chloritization is the dominant alteration observed along with sericitization and sausuritization (Fig.3e). The width of alteration zone varies from 1 to 3 m. It is ubiquitous to note that the alteration in the host rock is prominent along the S_2 cleavage planes indicating role of D_2 deformation. Naik (1984) has indicated development of fractures filled with mineralized quartz-carbonate veins during the Desani Granite emplacement especially during D_2 deformation.

Methodology

Rock samples were collected from the surface outcrops of quartzite, quartz-chlorite-actinolite schist and granite. Some subsurface samples were collected from drill core and mine dump. Thin sections and polished sections were prepared and petrographic study was carried out using research grade polarising optical microscopes available at NCEGR, GSI, Bangalore.

The X-ray diffraction (XRD) analyses (powder method) of selected samples were carried out on a PAN analytical X' Pert PRO-DY2006 diffracto-meter at the GSI laboratories in Bengaluru. The chemical compositions of chlorites were quantitatively determined by Electron Microprobe Analyzer (EPMA-CAMECA SX-100-WDS) in NCEGR laboratory, Bangalore. The fluid inclusion studies were carried out on Linkam THMSG-600 heating-freezing stage mounted on a fully equipped Olympus BX-50 transmitted light microscope at National Centre of Excellence for Geoscience Research (NCEGR), Geological Survey of India (GSI), Bangalore. Long working distance objective lenses, video camera and monitor, video graphics overlay with frame grabber and a fully programmable temperature controller. The maximum range of heating stage is up to 600° C (with water circuit) and freezing temperature is up to -195° C with a cooling media of liquid nitrogen.

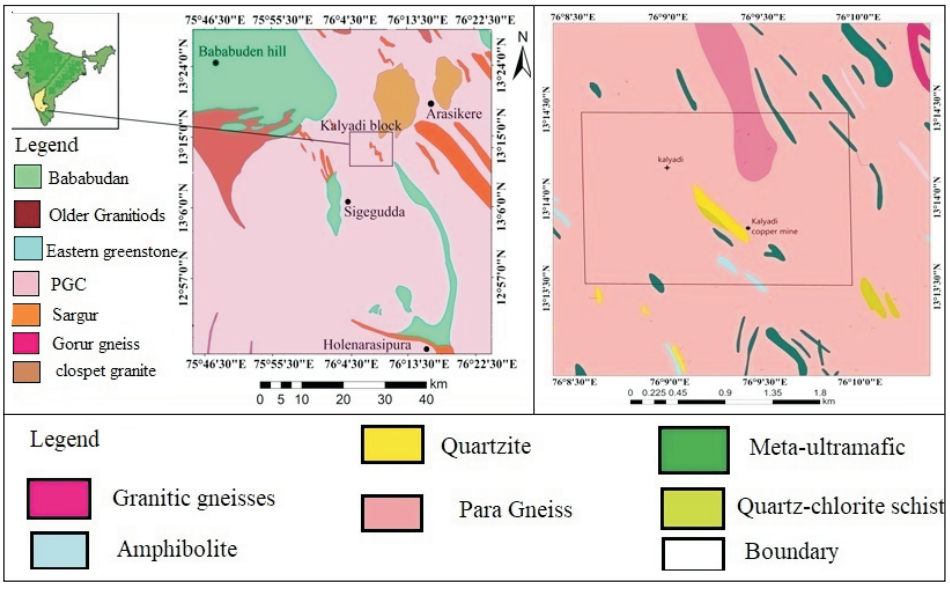

Fig.1. a) Location map of Kalyadi copper deposit and major schist belts of western Dharwar Craton; b) Geological map of Kalyadi schist belt western Dharwar Craton south India (*Modified after* Narasimhan and Viswanatha, 1970)

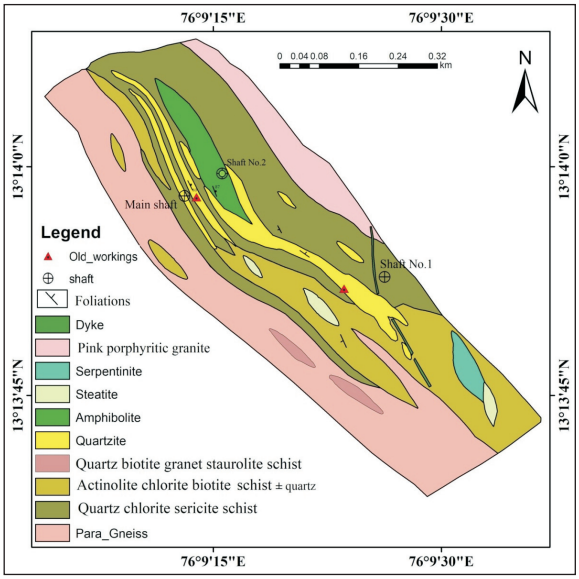

Fig.2. Detailed geological map of Kalyadi copper deposit (*Modified after* Ravidra *et al.*, 1990)

The stage was periodically calibrated by pure (demineralised) water (H_2O melting point=0°C) and pure CO_2 inclusions (synthetic CO_2 standard supplied by the stage manufacturer whose triple point = -56.6°C). Estimated accuracy was ±0.1°C at temperatures below 30°C and ±1.00°C at temperatures above 30°C. Reproducibility of the results of heating above 300°C has been tested and found to be ± 2 to 3°C.

Results

Petrography

Samples from the mineralized zone and the host rocks were subjected to petrographic studies covering mainly quartzites and metavolcanics. The quartzite shows fine grained nature and exhibits granoblastic texture at places (Fig.3c). Laminations and bedding is also present. Metavolcanic rocks contain quartz, biotite, actinolite, chlorite, plagioclase association with well-developed schistosity defined by mafic minerals. Evidence of shearing is recorded in host rock quartzite and metavolcanics, resulting in development of stretching, sub-grain formation, grain size reduction and marginal granulation (Fig.3e). Both the host rock contains mineralized quartz-carbonate veins. Chlorite is seen associated with Co mineralization and quartz carbonate veins (Fig.3f). At least two generation of chlorite can be deciphered related to the host rock as well as hydrothermal activity (Fig.3f). Chloritisation of biotite is very prominent in the rock. The composition of both the chlorites is petrologically almost same. Apart from chlorite, muscovite and epidote are also recorded resulting from either retrograde metamorphism or hydrothermal alteration. Ore mineral studies from the mineralized zones indicate presence of magnetite, chalcopyrite, pyrite, pyrrhotite, arsenopyrite and at places sphalerite. In general these sulphides are occurring as disseminations, stringers and fracture fillings in both the host rock (Fig.3f). Textural relationship between ore to ore and gangue minerals in the host rock indicates multistage mineralization in the area. Sulphides associated with calcite-quartz veins occur as late fracture filling (Fig.3i). Magnetite is the earliest phase present, showing typical idiomorphic texture. The magnetite is being replaced by later sulphides such as both chalcopyrite and pyrite.

The textural relationship between different sulphides and the mineral assemblage indicate at least two generation of chalcopyrite in the studied samples. In the first stage of mineralization chalcopyrite and pyrite ± arsenopyrite are formed. In the initial stage itself the chalcopyrite crystallized first followed by arsenopyrite and pyrite. This can be explained by the presence of euhedral pyrite sharing sharp margin replacing the early chalcopyrite (Ccp1) (Fig.3g). The second generation chalcopyrite (Ccp2) is characterized by replacement texture with early pyrite (Fig.3i). Fracture filling nature of chalcopyrite and re-absorbed margin in the pyrite further support this view. Arsenopyrite is generally euhedral to subhedral being replaced by chalcopyrite (Ccp2) at places (Fig.3h). Arsenopyrite and pyrite are not seen associated together, but may be derived from the same event owing to their replacement texture with late chalcopyrite. The second generation chalcopyrite is seen associated with pyrrhotite and both show mutual or common boundary texture, indicating their coeval nature. Presence of native Bi is recorded during the SEM-EDS studies seen as fracture filling along with Chalcopyrite (Ccp2) in pyrite indicating their association with second stage of mineralization (Fig.3j-k).

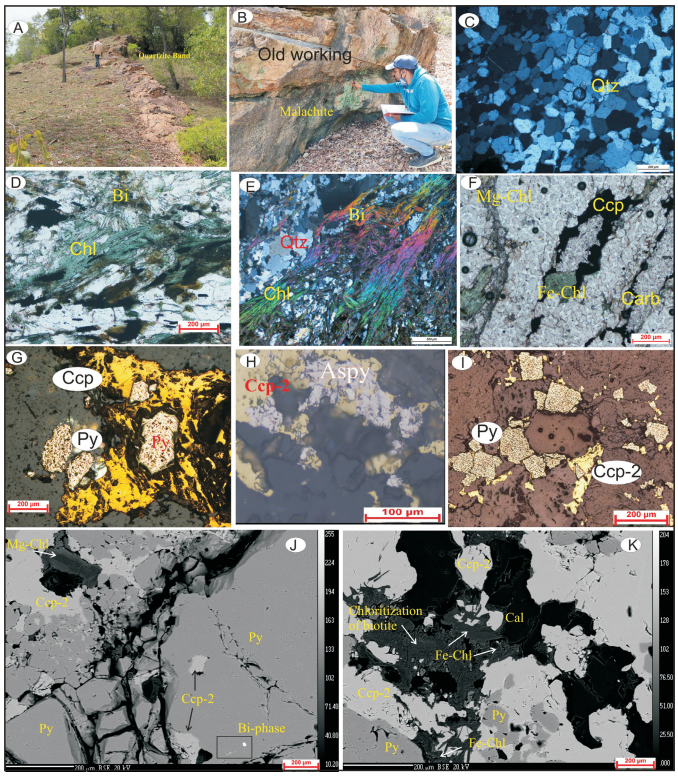

Fig.3. Field characteristics and mineralisation in Kalyadi area: (a) Field photographs of mineralized Quartzite band occur as long lenticular body runs almost 1 km strike length along NNW–SSE at Belliguthi hill, kalyadi area; (b) Field evidences of encrustation Malachite near old workings; (c) Photomicrographs of mineralized quartzite shows Granoblastic texture; (d) Showing chloritisation of biotite associated with sulphide mineralization; (e) Deformed quartz–chlorite veins showing S–C fabric;(f) Hydrothermal Fe-chlorite association with mineralized quartz-carbonate veins in quartz chlorite schist; (g) Early chalcopyrite (xenomorphic texture) replacing pyrite; (h) Chalcxopyrite-2 replacing arsenopyrite in KCD; (i) Chalcopyrite-2 replacing euhedral pyrite; (j) SEM-BSE images showing pyrite and chalcopyrite association and also shows native bismuth within the chalcopyrite; (k) Quartz-carbonate and Chlorite association with sulphides mineralization of KCD.

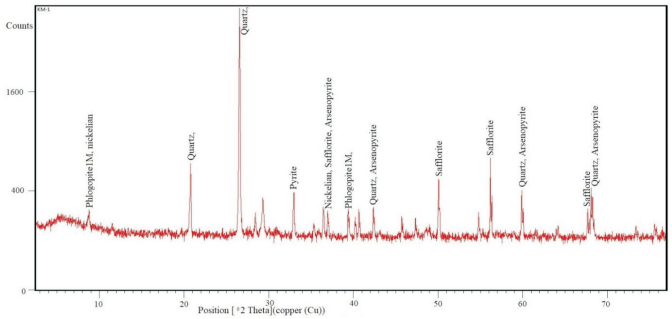

Fig.4. XRD patterns of b2 µm bulk sample fraction from hydrothermal alteration zone showing reflections of different polytypes at KCD. Figure shows X-ray diffraction patterns showing peaks for Safflorite [(Co, As) As2], Arsenopyrite, Nickelian, and quartz.

Earlier studies have shown the presence of Co in association with pyrite, which is seen in the both phases of mineralization. Stringers of chalcopyrite are present in the calcite-quartz veins and they represent the second phase. As the chalcopyrite is seen replacing pyrite, the Co concentration is also associated with them. There are no separate cobalt phases observed during the petrography. However significant concentration of safflorite (Co, As) As_2 associated with Nickelian, arsenopyrite and pyrite is recorded in the samples during XRD analysis (Fig.4).

EPMA Studies

Chlorite Chemistry and Thermometry

Chlorites analysed from the samples are mainly Fe rich in nature with Fe content varies from 0.59 to 0.89. When plotted onMgO-FeO-Al_2O_3 and Mg-Fe-Al total ternary diagrams, they show affinity towards Pseudo Thuringite, Dephanite and Chamosite. Two distinct clustering of data is observed which is reflected by variation in Mg and Fe concentration (Fig.5a-b). These clusters suggest two stages of chlorite development in the area. Early chlorite is characterized by relatively high Mg content in comparison with the late chlorite (Fig.5c-d). Hydrothermal origin in inferred for both the chlorites supported by petrography and associated mineral assemblage. Slightly Mg rich chlorite shows temperature ranging between 157.9 to 307.3° C, whereas low Mg chlorite shows temperature range varying from 202.8 to 322.43° C. Temperature data of both chlorites show large variation in lower temperature and not much or feeble variation in higher temperature range. No variation in higher temperature probably indicates overprinting of later thermal event on the early formed chlorite.

The estimated temperature of chlorite from three empirical methods is presented in table (Table 1-2). The results reveal that the lowest temperature is from T-1 as per the formula of Zang and Fyfe (1995), whereas the highest temperature obtained is from T-3 (Cathelineau and Nieva, 1985). The appropriate geothermometer selections depends on Fe and Mg content in the chlorite and those of chlorite used in the calibration of geothermometers as suggested by Klein *et al.* (2007). The T-3 (Cathelineau and Nieva, 1985) yielded a temperature range 261 to 577°C (mean 465°C), T-2 (Kranidiotis and MacLean, 1987) equation yielded a temperature ranges from 164 to 331°C (mean 267°C) which is similar to geothermometer T-1 (Zang and Fyfe, 1995) and it is matching with fluid inclusion homogenization temperature of the associated mineralised quartz veins. Hence, the geothermometer T-1 (Zang and Fyfe, 1995) is used in the present study.

Fluid Inclusion Study

Fluid inclusions were examined from the mineralized quartz vein samples collected from the ore zones of the KCD**.** Inclusions of both primary and secondary in nature were carefully selected for microthermometry following standard criteria (Roedder, 1984). Fluid inclusion petrography was done to identify fluid inclusion assemblages (FIA) in the mineralized quartz vein. Inclusions were identified and categorized on the basis of their identifiable phases such as aqueous vapour, aqueous liquid and carbonic liquid phases under transmitted light microscopy. The measurement were taken during ice melting include initial and final melting temperature of ice to determine the salinity and composition of the inclusions. During the heating of the fluid inclusions, homogenisation temperatures of CO_2 (Th CO_2) and total homogenisation temperature (T_h total) of aqueous bi phase inclusions were recorded. Calculation of density, salinity and plotting of the isochores coupled with the temperature and pressure estimates were carried out by using Linksys software (version 1.8) and also FLUIDS (Bakker, 2003).

Two distinct types of inclusions are observed during petrographic examination closely associated with the mineralization (Fig.6). In general the inclusion sizes are relatively smaller in size varying between 1 to 50 microns. Inclusions are monophase and biphase in nature having liquid and vapour phases (Fig.6c). The inclusions are irregular, euhedral faceted, rounded to oval shaped, which at places show effect of deformation (necking effect). Inclusions are either isolated or occur as trails which can be classified as FIA-I and II.FIA-I represent isolated inclusions at places and show crude alignment of both monophase and biphase inclusions (Fig.6d). FIA-II is occurring as trails of inclusion containing both monophase and biphase inclusions (Fig.6a-b).

Inclusions from both FIA are subjected to microthermometric

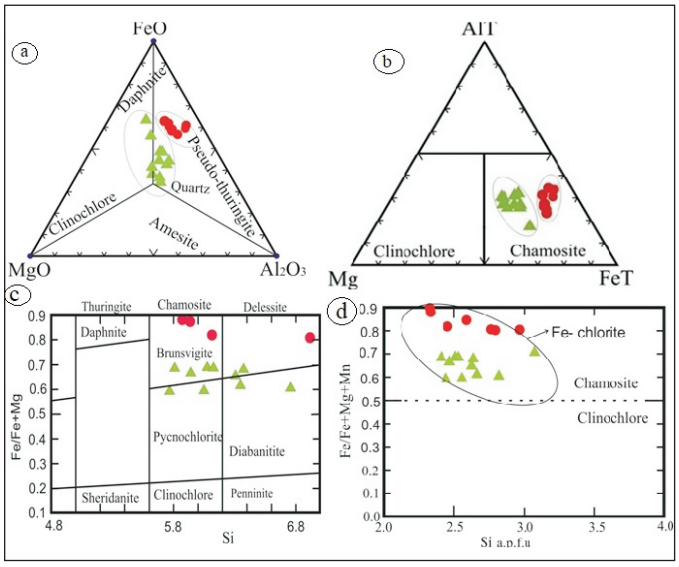

Fig.5. (a-b) Compositional variation diagram of the chlorite from (surface and subsurface samples) KCD, (a) based on the major oxide; (b) chamosites from the TCD (*after* Zane and Weiss, 1998); (c-d): Mineral composition of chlorite at KCD, c) Nomenclature and classification of chlorite at KCD (*after* Hey, 1954), (d) Classification of Kalyadi chlorite (*after* Bayliss, 1975).

Table 1: Summarized electron microprobe analysis of chlorite from surface and subsurface mineralized zone at Kalyadi copper deposit.

Sample No.	S4	S4	S2	S2	MS	MS	MS	MS1	MS2	FF-6	FF-6	FF-6	B-3	B-3	B-3	DC-1	RS-36	RS-36
Sample type	Qtz-chlorite vein in contact btw quartzite and metavolcanics		Quartz-chlorite- biotite schist															
SiO_2	24.64	24.01	22.67	22.38	26.86	24.36	26.25	26.31	27.42	26.54	24.79	25.06	24.42	30.33	25.14	31.15	27.03	25.45
TiO_2	0.03	0.05	0.08	0.07	0	0.04	0	0.04	0.02	0.04	0.02	0.02	0.13	0.54	0.07	0	0.04	0.07
Al_2O_3	20.7	21.22	20.95	20.57	14.91	19.72	11.7	15.47	12.55	16.7	17.31	17.56	17.58	20.14	21.64	10.25	17.19	16.94
FeO	25.83	26.84	37.03	37.77	33.7	35.1	31.36	32.8	30.63	28.84	29.53	29.06	21.5	21.96	21.87	32.81	24.59	25.46
MnO	0.1	0.14	0.19	0.22	0.23	0.08	0.13	0.19	0.18	0.33	0.31	0.28	0.15	0.14	0.12	0.06	0.61	0.79
MgO	14.17	13.24	4.49	3.77	7.53	7.25	6.88	7.22	6.5	14.2	13.89	13.85	17.66	16.94	18.65	13.16	17.61	14.72
CaO	0.03	0.08	0.03	0.09	0.24	0.02	0.68	0.65	0.9	0.08	0.03	0.01	0.01	0.01	0	0.32	0.01	0.06
Na_2O	0.02	0.04	0.03	0	0.07	0.02	0.05	0.02	0.04	0.2	0	0	0.02	0	0.02	0.02	0	0.02
K_2O	0	0	0.03	0.05	0.05	0.15	0.01	0.02	0.1	0.15	0.02	0.05	0.11	0.36	0.02	0.06	0.01	0.1
Cr_2O_3	0.08	0.13	0	0	0	0.01	0.03	0.06	0.18	0	0	0	0	0	0	0	0.02	0.03
NiO	0	0.11	0	0	0.12	0.02	0.05	0.14	0.28	0	0	0	0	0	0	0	0	0
Cation calculation based on 14 Oxygen																		
Si	2.47	2.41	2.33	2.33	2.80	2.46	2.97	2.77	3.02	2.64	2.51	2.53	2.56	2.82	2.44	3.08	2.66	2.62
Al iv	2.65	2.73	2.87	2.86	2.05	2.62	1.75	2.14	1.82	2.14	2.27	2.29	2.33	2.36	2.65	1.32	2.15	2.24
Al vi	0.00	0.00	0.00	0.00	0.00	0.00	0.00	0.00	0.00	0.00	0.00	0.00	0.00	0.00	0.00	0.00	0.00	0.00
Ti	0.00	0.00	0.01	0.01	0.00	0.00	0.00	0.00	0.00	0.00	0.00	0.00	0.01	0.04	0.01	0.00	0.00	0.01
Cr	0.01	0.01	0.00	0.00	0.00	0.00	0.00	0.00	0.02	0.00	0.00	0.00	0.00	0.00	0.00	0.00	0.00	0.00
Fe^{3+}	2.16	2.25	3.19	3.29	2.94	2.96	2.97	2.89	2.83	2.40	2.50	2.45	1.88	1.71	1.78	2.71	2.03	2.20
Fe^{2+}	0.00	0.00	0.00	0.00	0.00	0.00	0.00	0.00	0.00	0.00	0.00	0.00	0.00	0.00	0.00	0.00	0.00	0.00
Mn	0.01	0.01	0.02	0.02	0.02	0.01	0.01	0.02	0.02	0.03	0.03	0.02	0.01	0.01	0.01	0.01	0.05	0.07
Mg	2.12	1.98	0.69	0.58	1.17	1.09	1.16	1.13	1.07	2.10	2.10	2.09	2.76	2.35	2.70	1.94	2.58	2.26
Ni	0.00	0.01	0.00	0.00	0.01	0.00	0.00	0.01	0.02	0.00	0.00	0.00	0.00	0.00	0.00	0.00	0.00	0.00
Zn	0.00	0.00	0.00	0.00	0.00	0.00	0.00	0.00	0.00	0.00	0.00	0.00	0.00	0.00	0.00	0.00	0.00	0.00
Ca	0.00	0.01	0.00	0.01	0.03	0.00	0.08	0.07	0.11	0.01	0.00	0.00	0.00	0.00	0.00	0.03	0.00	0.01
Na	0.01	0.02	0.01	0.00	0.03	0.01	0.02	0.01	0.02	0.08	0.00	0.00	0.01	0.00	0.01	0.01	0.00	0.01
K	0.00	0.00	0.01	0.01	0.01	0.04	0.00	0.01	0.03	0.04	0.01	0.01	0.03	0.09	0.00	0.02	0.00	0.03
Fe/Fe+Mg	0.51	0.53	0.82	0.85	0.72	0.73	0.72	0.72	0.73	0.53	0.54	0.54	0.41	0.42	0.40	0.58	0.44	0.49
Aliv corrected	2.55	2.60	2.49	2.45	1.76	2.32	1.45	1.85	1.52	2.01	2.13	2.16	2.31	2.33	2.64	1.15	2.10	2.14
Temp(T_1)	299	307	322	321	235	296	203	245	210	245	258	261	265	268	299	158	246	255
Temp(T_2)	304	312	331	330	242	303	210	252	218	250	264	266	269	272	302	164	250	260
Temp(T_3)	558	569	545	538	390	510	325	409	339	445	469	475	508	511	577	261	464	472

Table 2: Electron microprobe analyses of chlorite from KCD and estimated temperature of chlorite formation using different empirical formulae.

Sl. No	Methods	Authors	Parameter used	Formulae used in estimation of chlorite temperature by using corrections factor	Temperature of chlorite from Host rock
1	Empirical methods	Zang and Fyfe (1995)	Al^{iv} and Fe / Fe + Mg	T (°C) = 106.2 Al_c^{iv} + 17.5 where $Al_c^{iv} = Al^{iv}$ - 0.88 [Fe / (Fe + Mg) - 0.34]	158 to 322°C (mean 260°C)
2		Kranidiotis and MacLean's (1987)	Al^{iv} and Fe / Fe + Mg	T (°C) =106Al^{iv}C +18 Where $Alc^{iv} = Al^{iv}$+ 0.7XFe	164 to 331°C (mean 267°C)
3		Cathelineau and Nieva (1985)	Al^{iv}	T = (0.0826 + Al^{iv}) / 0.00471	261 to 577°C (mean 465°C)

studies and observed two distinct compositions. Based on composition they can be classified as Type-I Aqueous-NaCl and Type-II carbonic inclusions, which are further detailed below.

Type I: H_2O-NaCl Inclusions

These are both monophase and biphase aqueous inclusions and are of varying size and shape, with a clear vapour bubble in liquid in case of biphase inclusions at room temperature (25° C). Their size commonly varies from 3 to 56 µm with irregular, faceted, rounded to oval shape. The total salinity range for the studied inclusions varies from 2.79 to 25.47 wt % NaCl equivalents to density values ranging from 0.816 to1.106 gms/cm^3(Table 3).Temperature of homogenization (T_h) varies from +148 to +258° C (Fig.7a). The inclusion composition contains NaCl and KCl in the fluid system which is based on the eutectic temperatures recorded i.e. -28 to -42° C (Bodnar, 1983; Zhang and Frantz, 1987; Brown and Lamb, 1988).There is distinct change in T_h, salinity and density of inclusions from both FIA-I and II (Fig.7c). However, the T_e is almost similar for both the FIA. The FIA-I shows T_h ranging from 171 to 258° C and salinity varying between 2.79 to 6.67 wt % NaClequivalents (Fig.8b). The density of FIA-I is < 1 gms/cm^3 i.e. 0.81 to 0.93 gms/cm^3. The FIA-II shows T_h ranging from 148 to 198° C and salinity varying between 21.66 to 25.47 wt % NaCl equivalents. The density of FIA-II is > 1 gms/cm^3 i.e. 1.05 to1.11gms/cm^3.

Type II: C_2 Inclusions

Carbonic inclusions are monophase in nature and shows similar composition in both FIA. They occur both as trails and isolated inclusions. The temperature of CO_2 melting of carbonic fluid inclusions ranges from -62°C to -65°C indicating admixtures of other phases with CO_2. The presence of CH_4 can be inferred from depreciating *T*m of CO_2. The homogenization temperature ranges from -1°C to +2.1° C. The density of carbonic inclusions varies from 0.91 to 0.93gms/cm^3.

Pressure – Temperature Conditions of Entrapment

The P-T conditions of entrapment of fluid inclusions can be obtained by intersecting isochores (Roedder and Bodnar, 1980) was adopted with help of coeval inclusions, assuming synchronous entrapment and no post- modification changes in the inclusions. Four intersection points (1.9kbar/268°C, 2.3kbar/298°C, 1.9kbar/162°C and 1.9kbar/224°C) pertaining to the ore fluids P-T were obtained. In addition, pressure values were further constrained

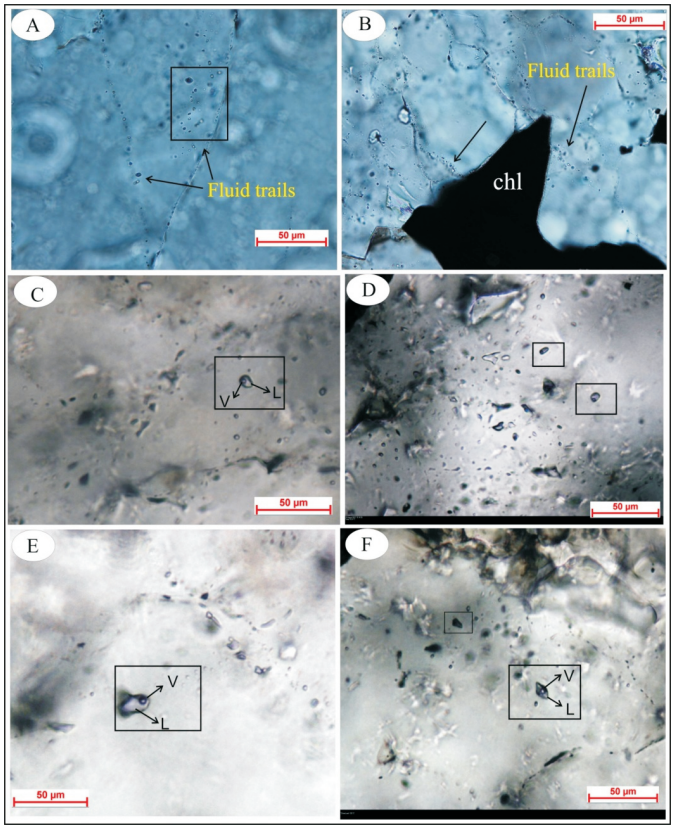

Fig.6. Photomicrographs of mineralized quartz vein and different inclusion types from kalyadi copper deposit; (a-b) showing fluid inclusion trails; (c) primary aqueous bi-phase inclusions, (d) primary mono-phase and bi-phase aqueous inclusions, (e-f) primary trails of mono-phase and bi-phase inclusion.

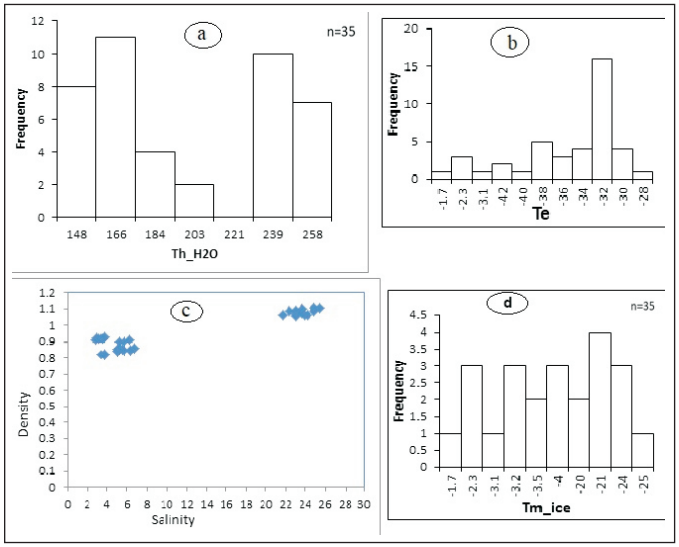

Fig.7. Histograms for aqueous biphase inclusions from mineralized quartz carbonates veins. a) Showing Th (temperature of homogenization) of FIA-I and FIA-II; b) Te of biphase inclusions; c) Binary diagram plotted on salinity *vs* Density of fluids; d) Temperature of last ice melting.

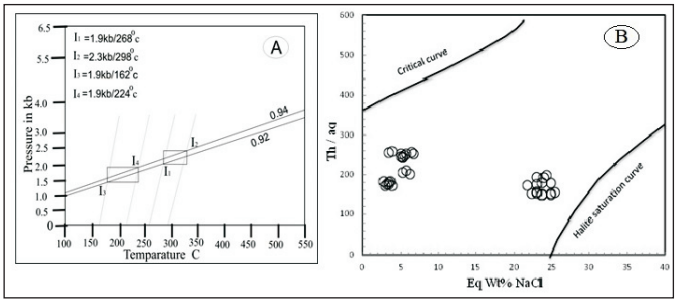

Fig.8. Intersecting isochores of type-I and Type –II inclusions from mineralised quartz –carbonate veins at KCD using FLUIDS software (Bakker, 2003). A) The squares correspond to P and T obtained from the aqueous-carbonic inclusionsare from the intersection points; B) Plots of inclusions in Temperature of homogenisation vs. salinity filed.

at the temperatures obtained from chlorite thermometry. For this purpose, the total range in average temperature (203 to 322° C) from chlorite data, upon intersection with the isochores of type-I fluid inclusions furnished a pressure range of 1.9 to 2.3 Kbar (Fig. 8a). Therefore, the thermobarometry pursued by the above two independent approaches yielded comparable P-T values, thus, further justifying the isochores intersection method used in this study.

Discussion

Understanding the genesis of any mineralization require extensive work characterizing source, processes and trap site. In a Precambrian terrain, it will be more challenging to decipher this, considering multiple deformation and metamorphism. Unravelling the history of mineralization can be done through field and various laboratory techniques. Some of the common tools *viz.*, petrography, fluid inclusion study, XRD, mineral chemistry, stable isotope study are being used by the workers. In the Indian context, all the Precambrian Cratonic parts are well known for mineralization. In the Dharwar Craton, Cu, Au, PGE, Co, Ti-V etc mineralization is being reported from number of older Sargur supracrustal belts. Nuggihalli, Aladahalli and the KSB are typical Sargur equivalent schist belt known for Cu mineralization. Majority of the mineralization in these belts are directly or indirectly related to magmatic activity. In the present study, the KSB, which is an integral part of the Sargur Supracrustal Belt, is known for Cu mineralization (Cu up to 1 %), which is also being mined in the last two decades. Ravindra *et al.* (1990) have reported Co mineralization associated with Cu from this belt. Co values up to 2000 ppm is present associated with Cu, which is quite high considering its strategic importance and non-availability of exclusive Co deposit elsewhere in India (Mahantesha *et al.*, 2021). Mahantesha *et al.* (2021) reported the presence of Co concentration up to 2000 ppm in Quartzite, up to 1200 ppm in metavolcanics and up to 500 ppm in the quartzo-feldspathic veins in quartzite in this belt.

In the KSB, earlier workers have given importance to copper mineralization and its genesis. Subba Rao and Naqvi (1997) have studied associated copper mineralization primarily with Stratiform and strata bound type hosted mainly with metachert derived from a submarine exhalative source with subsequent enrichment of fluids derived from granitic activity. Though, Cu and Co are closely associated, it is still not clear about the Co genesis. Mahantesha *et al.* (2021) have tried to interpret genesis of Co based on petrography and geochemistry. They have opined that the Co mineralization is associated with structurally controlled quartz carbonate vein. Fluids associated with granitic activity played role in remobilization of mineralization. Both the evidences have highlighted role of fluids associated with granitic activity, which in this case is the Desani Granite emplaced during D2 deformation.

Table 3: Fluid inclusion data of representative samples of mineralised quartz veins from KCD.

Inclusion no.	Incl type	Te	Tm ice	Th_ aq	Tm CO_2	Th CO_2	Eq Wt% Nacl	Density
1.	V+L	-38	-23	198	-	-	24.28	1.06
2.	V+L	-37	-22.5	192	-	-	23.98	1.06
3.	V+L	-35	-21	193	-	-	23.02	1.05
4.	V+L	-42	-3.2	205	-	-	5.17	0.90
5.	V+L	-41	-3.9	201	-	-	6.23	0.91
6.	V+L	-40	-3.5	252	-	-	5.62	0.84
7.	V+L	-38	-3.4	248	-	-	5.47	0.85
8.	V+L	-38	-3.1	245	-	-	5.01	0.85
10.	V+L	-32	-3.2	244	-	-	5.17	0.85
11.	V+L	-34	-3.5	210	-	-	5.62	0.90
12.	V+L	-35	-2.3	171	-	-	3.76	0.93
13.	V+L	-34	-2.1	175	-	-	3.44	0.92
14.	V+L	-38	-2.2	182	-	-	3.60	0.91
15.	V+L	-30	-4	256	-	-	6.37	0.84
16.	V+L	-32	-4.2	252	-	-	6.67	0.85
17.	V+L	-32	-24	178	-	-	24.89	1.08
18.	V+L	-30	-22	179	-	-	23.66	1.07
19.	V+L	-32	-21	156	-	-	23.02	1.09
20.	V+L	-30	-22	150	-	-	23.66	1.10
21.	V+L	-32	-20	152	-	-	22.35	1.08
22.	V+L	-34	-21	153	-	-	23.02	1.09
23.	V+L	-31	-24	149	-	-	24.89	1.11
24.	V+L	-32	-22	148	-	-	23.66	1.10
25.	V+L	-34	-24	152	-	-	24.89	1.10
26.	V+L	-32	-25	155	-	-	25.47	1.11
27.	V+L	-28	-2.3	258	-	-	3.76	0.82
28.	V+L	-29	-2.1	255	-	-	3.44	0.82
29.	V+L	-32	-3.1	252	-	-	5.01	0.84
30.	V+L	-30	-1.8	171	-	-	2.96	0.92
31.	V+L	-29	-1.7	182	-	-	2.79	0.91
32.	V+L	-30	-1.9	175	-	-	3.12	0.92
33.	V+L	-31	-2.1	180	-	-	3.44	0.91
34.	V+L	-31	-19	172	-	-	21.66	1.06
35.	V+L	-29	-21	175	-	-	23.02	1.07
36.	L	-	-	-	-65	1.2	-	0.92
37.	L	-	-	-	-64	1.9	-	0.92
38.	L	-	-	-	-62	1	-	0.92
39.	L	-	-	-	-63	1.5	-	0.92
40.	L	-	-	-	-62	2.1	-	0.92
41.	L	-	-	-	-63	-2	-	0.94

Ore petrographic studies reveal two generation of chalcopyrite based on textural relationship. The chalcopyrite, pyrite and arsenopyrite association defines first stage followed by chalcopyrite, pyrrhotite, native Bi and safflorite. Co is seen in both the assemblages. In the initial stage Co is associated with pyrite and chalcopyrite in their crystal lattice (Thomas, 2006) and in the second stage Co is occurring as arsenide phase *i.e.* safflorite - (Co, As) As_2. Fluid inclusion studies also support a two stage mineralization event in the area based on salinity and density of fluids with dominant H_2O-NaCl-KCl system. Two distinct clustering of data is observed in the salinity *vs* T_h and salinity *vs* density diagram, further supports two stage evolution. There is no evidence of boiling, thus T_h is not the actual temperature of entrapment of these mineralizing fluids. The isochores intersection method has yielded temperature range of 268° to 300° C for initial fluids with pressure range from 1.9 to 2.3 Kb, whereas the second

generation of fluids show temperature range 162° to 224° C with the pressure ranging from 1.4 to 1.9 Kb.

The initial stage fluids are characterized by low saline (~ 5 wt % NaCl equivalent) slightly higher temperature (268° to 300° C), which are almost similar to temperatures obtained from the chlorite *i.e.* 202.8 to 322.43° C. These temperature and pressure range along with low salinity indicates that these fluids are related to regional low grade green schist facies metamorphism. The Co was initially associated with mafic-ultramafic rocks of the belt having good concentration of Co *i.e.* up to 1200 ppm in the metavolcanic rock (quartz chlorite schist).Further, the Sulphur isotope compositions of chalcopyrite from Kalyadi show near zero $\delta^{34}S$ (- 0.8 %), indicative of a magmatic source of possible mantle origin (Safonov *et al.*, 1980; Menon *et al.*, 1981; Vasudev, 1983). Mg rich nature of Fe-chlorites are also support this view. The first phase fluids have played important role in remobilization of Co along with Cu and re-concentration and redistribution of the same in both metavolcanic and quartzite as quartz-carbonate veins. On the contrary, the late stage fluids are characterized by high density and high saline nature suggesting their derivation from the granitic or felsic magmatic source. Presence of safflorite mineral associated with the second stage fluids and mineral assemblage suggests that the remobilization Co from the crystal lattice of pyrite, chalcopyrite is indicated. This is a first report of a separate cobalt mineral phase occurrence from the Kalyadi copper deposit. This is further supported by the presence of Desani intrusive granite in the area and also the quartzo-feldspathic veins in the quartzite having good concentration of Co (*i.e.* up to 500 ppm). Presence of native Bi associated with second stage chalcopyrite further support a felsic magmatic source.

Conclusions

The cobalt mineralization in the KSB is associated with quartzite and metavolcanic rock (quartz-chlorite schist). In general, Co mineralization in the KSB is epigenetic and epithermal in nature associated with two stage hydrothermal activity. Early stage mineralization associated with pyrite and later as separate phase of Co, *i.e.* Safflorite [(Co, As), As2]. The fluid entrapment temperatures (162 to 300° C), salinities and chlorite chemistry further supports two stage evolution of Co mineralization in the Kalyadi area. Role of the Desani Granite in the remobilization of Co in the second stage is evident from the field, petrography and fluid inclusion studies.

Authors' Contributions

Mahantesha P: Investigation, Conceptualization, Methodology, Software, Writing - Original Draft. **K. N. Prakash Narasimha:** Supervision and Editing**. Md. shareef:** Visualization, Writing - Reviewing and Editing. **G. Gopalakrishna:** Reviewing. **Girish Kumar Mayachar:** Formal analysis. **S.S.A. Rasool:** Formal analysis**. Aneesh S.S:** Formal analysis. **T.K.A. Rahim:** Visualization and Reviewing.

Conflict of Interest

Authors declare no conflict of interest.

Acknowledgments

The author express sincere gratitude to the Chairman of the Department of Earth Science and the Chairman, Board of Studies in Earth Science, University of Mysore, Mysore for the constant support and encouragement during the studies. Author is profusely thankful to the Deputy Director General, and officers of Chemical Division, GSI, Bangalore, for providing analytical facilities. We also acknowledge and express sincere thanks to the personnel of EPMA and XRD Laboratory, GSI, Bengaluru as well for analysing the samples.

References

Abdul Rahim T.K. and Nijagunappa, R. (2001). Mineragraphy of sulphide mineralisation in Kalyadi copper mine~ Hassan district, Karnataka. Miner. Deposit., v. 32, 220p.

Bakker, R.J. (2003). Package FLUIDS 1. Computer programs for analysis of fluid inclusion data and modeling bulk fluid properties. Chem. Geol. 194, pp. 3–23.

Bayliss, P. (1975). Nomenclature of the trioctahedral chlorites. Can. Mineral., v. 13, pp.178–180.

Bhaskar Rao, B. and Venkataraman, S. (1982). Geochemistry and genesis of Archean meta- volcanic rocks from a part of the Nuggihalli schist belt, Hassan district, Karnataka, India. Brasil. Geosci., v.12 (1-3), pp. 375-379.

Bodnar, R.J. (1983). A method of calculating fluid-inclusion volumes based on vapor bubble diameters and P-V-T-X properties of inclusion fluids. *Eco. Geol.,* v. 78, pp. 535-542.

Brown, P.E. and Lamb, W.M. (1988). P-V-T properties of fluids in the system H_2O-CO_2-NaCl: New graphical presentation and implications for fluid inclusion studies. *Geochim. Cosmochim. Acta, v.* 53, pp.1209-21.

Cathelineau, M. and Nieva, D. (1985). A chlorite solid solution geothermometer. The LosAzufres(Mexico) geothermal system. Contrib. Mineral. Petrol., v. 91, pp. 235–244.

Dora, M.L., Randive, K.R. and Ramachandra, H.M. (2017). Iron oxide–copper–gold mineralization at Thanewasna, western Bastar Craton. Curr. Sci., v. 112(5), pp.1-10.

Hey, M.H. (1954). A new review of the chlorites. Mineral. Mag. 30, pp. 277–292.

Kranidiotis, P. and Maclean, W.H.S. (1987). Systematic of chlorite alteration at the Phelps Dodge massive sulfide deposit, Matagami, Quebec. Econ. Geol., v. 82, pp. 1898–1911.

Krishna Rao (1998). Strategy for the benefeciation of ores of some strategic metals in India. Metal. Mater. Process., v.10(1), pp.21-40.

Klein, E.L., Harris, C., Giret, A. and Moura, C.A.V. (2007). The Cipoeiro gold deposit, Gurupi Belt, Brazil: Geology, chlorite geochemistry, and stable isotope study. Jour. South. Am. Earth Sci. v.23, pp.242–255.

Menon, A.G., Venkatasubramanian, V.S. and Anantha Iyer, G.V. (1981). Sulphur isotope abundance Variations in sulphides of the Dharwar Craton ± Part 1: Kalyadi. Jour. Geol. Soc. India, v. 22, pp. 391-398.

Mahantesha, P., Prakash, K.N., Narasimha, Md. Shareef, Gopalkrishna, G. and Rahim, T.K.A. (2021). Cobalt mineralisation associated with copper from Kalyadi area, western Dharwar craton, south India. Jour. Geosci. Res., v.6(2), pp. 134-146.

Mookherjee, A. and Philip, R. (1979). Distribution of copper, cobalt and nickel in ores and host rocks, Ingaldhal, Karnataka,

India. Miner. Deposit., v.14, pp. 33-55.

Naik, M.S. (1984). Granite magmatism and copper mineralisation at Kalyadi, Hassan district, Karnataka. Proc. Symp. Metallog. Precamb., IGCP Prog. 91. Geol. Surv. India, v. 22, pp. 153-166.

Narsimhan, M. and Viswanatha, M.N. (1970). Detailed investigation for copper ore in Kalyadi area, Hassan district, Mysore State. Geol. Surv. India. Unpublished report, pp. 153-166.

Nayak, Prasanta Kumar (2011). Cobalt-Bearing Grunerite in the Metamorphosed Banded Iron Formation in Orissa, India. *Resour. Geol., v*. 61(3), pp. 281–289.

Paremeswaraiah, K.S. (1996). Cobalt- a new economic metal in the mineral map of India. Proc. All India Sem. 'Mineral.Econ.India', the Institution of Engineers (India), Karnataka state center, mining engineering Division, Bangalore.

Ravindra, B.M., Krishna Rao, B. and Vasudev, V.N. (1990). Ore-petrological aspects of copper mineralisation near Kalyadi, Hassan district, Karnataka. Jour. Geol. Soc. India, v. 35, pp.159-172.

Roedder, E. (1984). Fluid Inclusions. Rev. Mineral. (Min. Soc. America), v. 12, 644p.

Roedder, E. and Bodnar, R.J. (1980) Geologic Pressure Determinations from Fluid Inclusion Studies. Ann. Rev. Earth Planet. Sci., v. 8, pp. 263-301. http://dx.doi.org/10.1146/annurev.ea.08.050180.001403

SubbaRao, D.V. and Naqvi, S.M. (1997). Geological setting, mineralogy, geochemistry and genesis of the Middle Archaean Kalyadi copper deposit, western Dharwar Craton, southern India Mineral. Deposit., v. 32, pp. 230-242.

Safonov, Y.G., Radhakrishna, B.P., Krishna Rao, B., Vasudev, V.N., Raju, K.K., Nosik, L.P., Pashkov,Y.N. (1980). Mineralogical and geochemical features of endogene gold and copper deposits of South India. Jour. Geol. Soc. India, v.21, pp. 365-378.

Thomas Jayasree (2006). Mineralogical and Electron Microprobe Studies on the Cobalt Sample from Kalyadi Copper Deposit, Hassan District, Karnataka. Proc. Internatl. Sem. Miner. Process. Technol., Chennai, India, pp. 149 - 156.

Vasudev, V.N. (1983). Geological evolution of Archaean and early Proterozoic sulphide deposits of the Dharwar Craton, India. *In*: Naqvi, S.M. and Rogers, J.J.W. (*Eds*.) Precambrian of South India. Geol. Soc. India Mem., 4, Bangalore.

Zang, W. and Fyfe, W.S. (1995). Chloritisation of the hydrothermally altered bedrock at the Igarapé Bahia gold deposit, Carajás, Brazil. Miner. Deposit., v. 30, pp. 30–38.

Zane, A. and Weiss, Z. (1998). A procedure for classifying rock-forming chlorites based on microprobe data. Rend. Fis. Acc. Lincei, v. 9, pp. 51–56

Zhang, Y.G. and Frantz, J.D. (1987). Determination of the homogenisation temperatures and densities of superficial fluids in the system NaCl-KCl-$CaCl_2$-H_2O using synthetic fluids inclusions. *Chem. Geol., v.* 64, pp. 335- 342.